EURO:TUN 2013
3rd International Conference on Computational Methods in Tunnelling and Subsurface Engineering
Ruhr University Bochum, 17-19 April 2013

Numerical analysis of swelling deformations in tunnelling – a case study

Bert Schädlich[1], Helmut F. Schweiger[1] and Thomas Marcher[3]
[1]Graz University of Technology, Rechbauerstraße 12, A-8010 Graz, Austria
[2]ILF Consulting Engineers, Feldkreuzstraße 3, A-6063 Rum / Innsbruck, Austria

Abstract

This paper presents a numerical analysis of swelling deformations in the Pfaendertunnel near Bregenz/Austria, which is a well-known example for swelling in claystones. The constitutive model used in this study employs a semi-logarithmic reduction of swelling strains with stress level and exponential convergence with final swelling strains over time. Input swelling parameters for the analysis were derived from laboratory swelling tests. Due to the wide range of experimental results, upper and lower bounds of swelling parameters were used in the analysis. Calculated invert heave was in particular sensitive to the choice of the maximum swelling pressure, which governs both the swelling strain at stress point level and the size of the swelling zone below the tunnel invert. Good match with the in situ measurements was obtained for a maximum swelling pressure of 1500 kPa, which represents the upper edge of the experimental values and is significantly lower than the overburden pressure of about 4900 kPa.

Keywords: Swelling rock, clay swelling

1 INTRODUCTION

Swelling phenomena have caused major difficulties in many tunnelling projects in the last 100 years. When water is allowed to infiltrate the swelling rock mass after tunnel excavation, chemical processes within the rock matrix can be initiated which result in large volume increase. As water aggregates at the tunnel invert, typically large invert heave deformations evolve if no or a flexible invert lining is installed. In the case of a rigid support concept, large swelling pressures may develop. The most prominent rock types exhibiting swelling behaviour are certain types of claystone and rocks containing anhydrite. This paper focusses on the derivation of calculation parameters from laboratory swelling tests in order to back analyse in situ measurements with a novel constitutive model for swelling rock.

2 SWELLING ROCK MODEL

As the details of the model (which has been implemented by T. Benz, NTNU Norway as a user-defined soil model for the finite element software PLAXIS) are unpublished as yet, the main features of the model are briefly explained in the following section.

2.1 Stress dependency of swelling

The relationship between final swelling strains $\varepsilon_i^{q(t=\infty)}$ and the axial stress in the direction of swelling is given by Grob's [2] semi-logarithmic swelling law (Figure 1).

$$\varepsilon_i^{q(t=\infty)} = -k_{qi} \cdot \log_{10}\left(\frac{\sigma_i}{\sigma_{q0i}}\right) \tag{1.}$$

k_{qi} is the (axial) swelling parameter, σ_i is the axial stress and σ_{q0i} is the maximum swelling stress in that direction. Swelling strains are calculated in the coordinate system of principle stresses without any interaction of swelling in the different directions [5].

2.2 Time dependency of swelling

The model is based on exponential convergence towards the final swelling strain with time [5]. The swelling strain increment is determined by the parameter η_q (Figure 1). The influence of elastic and plastic volumetric strains, ε_v^{el} and ε_v^{pl}, can be taken into

account by the parameters A_{el} and A_{pl}. Positive volumetric strains (loosening of the material) result in faster approach of the final swelling strain, while negative volumetric strains delay or may even stop the evolution of the swelling strains. This approach accounts for the dependency of the swelling rate on the penetration rate of water, which changes with the permeability of the rock mass.

$$\varepsilon_i^{q(t+\Delta t)} = \varepsilon_i^{q(t)} + \frac{\left(\varepsilon_i^{q(t=\infty)} - \varepsilon_i^{q(t)}\right)}{\eta_q(t)} \cdot \Delta t \tag{2.}$$

$$\eta_q(t) = 1/\left(A_0 + A_{el} \cdot \varepsilon_v^{el} + A_{pl} \cdot \varepsilon_v^{pl}\right) \tag{3.}$$

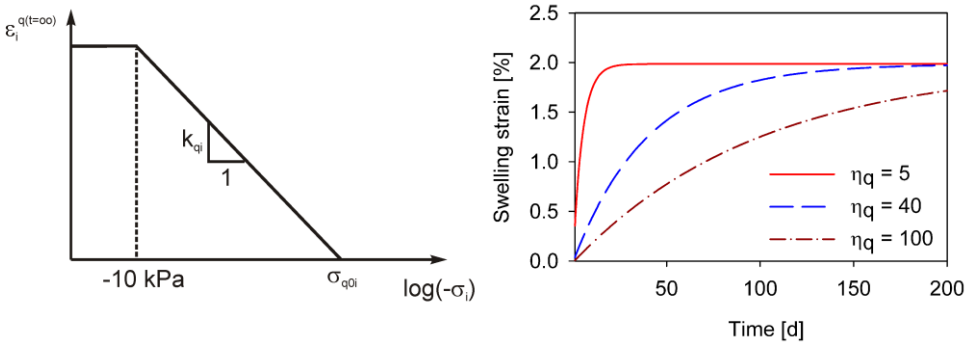

Figure 1: Semi-logarithmic swelling law and influence of η_q on evolution of swelling strains

2.3 Plastic strains and iterative procedure

Plastic strains are calculated according to a Mohr-Coulomb failure criterion with tension cut-off. Shear strength is defined by effective friction angle, φ', and effective cohesion, c'. The direction of the plastic strain increment is defined by a non-associated flow rule, using the angle of dilatancy ψ. The elastic, plastic and swelling strain increments add up to the total strain increment:

$$\Delta\boldsymbol{\varepsilon} = \Delta\boldsymbol{\varepsilon}^{el} + \Delta\boldsymbol{\varepsilon}^{pl} + \Delta\boldsymbol{\varepsilon}^{q} \tag{4.}$$

An implicit backward-Euler-scheme is used on stress point level to find the stress state which satisfies the constitutive equations for the given total strain increment.

3 PFÄNDERTUNNEL CASE STUDY

3.1 Project description

The 6.7 km long first tube of the Pfändertunnel near Bregenz (Austria) was constructed in 1976-1980 according to the principles of the New Austrian Tunnelling Method (NATM). The Pfänderstock consists of various sedimentary molasse rocks (sandstone, conglomerate, claystone, marl) which were deposited in the area north of the Alps. Significant invert heave of up to 30 cm was observed after about 75% of the tunnel length was excavated. These observations lead to detailed laboratory investigations of the swelling characteristics of the Pfaenderstock material, an extensive monitoring program and to the installation of additional anchors in the tunnel invert.

3.2 Laboratory swelling tests

The marl (claystone) layers were identified as the rock type causing the swelling of the tunnel invert due to their high content of Montmorillonite. Czurda & Ginther [1] reported results of swell heave tests in oedometric conditions, i.e. the evolution of vertical strain was monitored under constant vertical stress. They distinguished between undisturbed molasse marl (series A) and the fault zone material (series B, Figure 2). Series A samples showed higher maximum swelling potential, but lower maximum swelling pressures than the samples of series B.

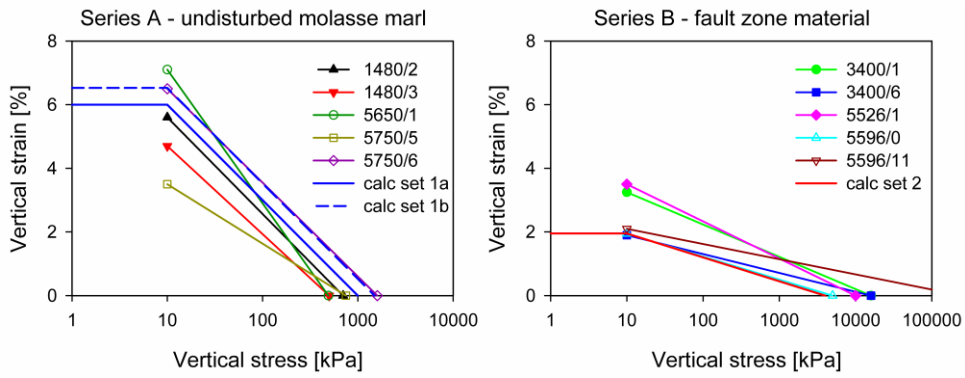

Figure 2: Swelling test results after [1]

This notable difference was attributed to relaxation and swelling of the series B samples before the samples could be tested [1]. For the back analysis two swelling parameter sets are considered, which represent the upper and lower boundary of the test results. The time swelling parameters A_0, A_{el} and A_{pl} are calibrated to match the in situ time-swelling curve.

3.3 Numerical model and material parameters

The 2D plane strain finite element model used in this study is shown in Figure 3. Tunnel geometry and basic material parameters of the marl layer (E = 2.5 GPa, ϕ' = 34°, c' = 1000 kPa) have been taken from [4]. Tunnel overburden is ~200 m above the tunnel crown, which is representative of the cross section at km 5+373. Linear elastic plate elements are used for the shotcrete lining, with E = 7.5 GPa for the young and E = 15 GPa for the cured shotcrete. The final concrete lining is modelled with volume elements assuming linear elastic behaviour and a stiffness of E = 30 GPa. The final lining thickness varies between 50 cm at the invert and 25 cm at the crown.
Swelling parameters are listed in Table 1 and illustrated in Figure 2. Sets 1a, 1b and 2a only employ A_0 for the time dependency of swelling, while in set 2b evolution of swelling with time is entirely governed by elastic volumetric strains.
After top heading / invert excavation (assuming pre-relaxation factors of 75% and 37.5%, respectively), the concrete invert arch is installed. Swelling is confined in the model to an area of 15 m x 15 m below the tunnel invert. After a swelling phase of 65 days, the final lining is activated, followed by another swelling phase of 115 days. John reported that the decision on invert anchoring and pre-stressing was based on the swell heave deformations observed up to this point [3]. In the cross section considered here this resulted in applying a pattern with 2.2 m anchor spacing.

Table 1: Swelling parameters

parameter	**set 1a**	**set 1b**	**set 2a**	**set 2b**
swelling potential k_q [%]	3.0	3.0	0.75	0.75
max. swelling stress σ_{q0} [kPa]	1000	1500	4000	4000
A_0	5.0e-3	2.5e-3	3.0e-3	0.0
A_{el}	0.0	0.0	0.0	9.0
A_{pl}	0.0	0.0	0.0	0.0

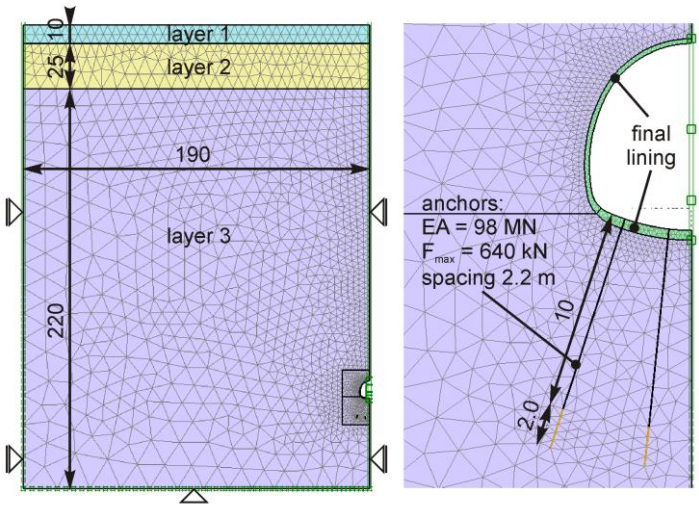

Figure 3: Finite element model (dimensions in [m])

3.4 Results

3.4.1 Evolution of invert heave with time

Figure 4 compares the time-swelling curves calculated with the different parameter sets with the measured invert heave in km 5+373 [3]. The measurements plot close to a straight line in logarithmic time scale, which cannot be reproduced exactly by the exponential approach employed in the model. The match with the measured invert heave is, however, sufficient from a practical point of view.

Set 1a delivers too little invert heave (10 mm), and the development of deformations completely stops after activating the prestressed anchors. Increasing the maximum swelling stress by 50% (set 1b) yields ~50% more deformation and a better match with the measurements. While such a significant influence may be expected, it should be noted that experimental results for these two sets plot so close to each other that either of the two parameter sets appears justified (Figure 2).

Surprisingly, sets 2a and 2b – which represent much smaller free-swell deformations – deliver more invert heave than sets 1a and 1b. This is a result of the higher maximum swelling stress of sets 2a and 2b, which activates swelling in deeper rock layers. Modelling the evolution of swelling with time entirely in dependence on elastic volumetric strains (set 2b) results in a slightly more prolonged time-swell-curve than using a constant value of A_0 (set 2a).

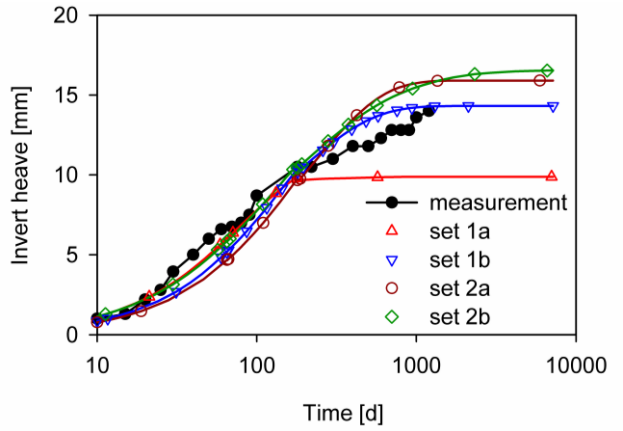

Figure 4: Development of invert heave with time

3.4.2 Distribution of swelling strains over depth

The size of the rock mass which is affected by swelling depends primarily on the maximum swelling stress. For set 1b (σ_{q0} = 1500 kPa) the swelling zone is confined to about 2 m below the tunnel invert, which matches well with the sliding micrometer measurements in cross section km 5+820 (Figure 5). The swelling zone with sets 2a and 2b (σ_{q0} = 4000 kPa) is much deeper due to the higher maximum swelling pressure, even though similar invert heave is obtained with both parameter sets.

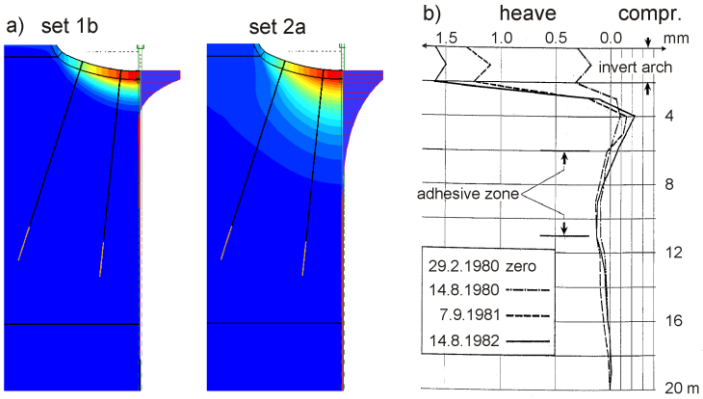

Figure 5: Profile of vertical displacements, a) numerical analysis at t = 7180 d, b) measurements km 5+820 [3]

4 CONCLUSIONS

This paper presented the results of a back analysis of measured swelling deformations in the Pfaendertunnel (Austria). A constitutive model based on Grob's swelling law and exponential convergence with final swelling strains over time was used for the numerical calculations. Input swelling parameters were derived from laboratory swelling tests.

Different sets of swelling potential k_q and maximum swelling stress σ_{q0} delivered very similar swelling deformations at the tunnel lining, as increasing σ_{q0} is roughly equivalent to increasing k_q. However, good match with the measured displacement profile below the tunnel invert was only obtained with σ_{q0} = 1500 kPa, which represents the upper edge of the experimental results on undisturbed molasse marl. Using higher values of σ_{q0} delivered too large swelling zones. The invert heave measurements plot close to a straight line in logarithmic time scale, which cannot be exactly reproduced by the exponential approach of the constitutive model. The match with the measured evolution of swelling, however, is sufficient from a practical point of view.

REFERENCES

[1] Czurda, K. A., and Ginther, G.: Quellverhalten der Molassemergel im Pfänderstock bei Bregenz, Österreich. Mitt. österr. geolog. Ges. 76 (1983), 141-160.

[2] Grob, H.: Schwelldruck im Belchentunnel. Proc. Int. Symp. für Untertagebau, Luzern (1972), 99-119.

[3] John, M.: Anwendung der neuen österreichischen Tunnelbauweise bei quellendem Gebirge im Pfändertunnel. Proc. of the 31st Geomechanik Kolloquium, Salzburg 1982.

[4] John, M., Marcher, T., Pilser, G., and Alber, O.: Considerations of swelling for the 2nd bore of the Pfändertunnel. Proc. of the World Tunnel Congress, Budapest 2009, 50-61.

[5] Wittke-Gattermann, P., and Wittke, M.: Computation of Strains and Pressures for Tunnels in Swelling Rocks. Proc. ITA 2004 E14, 1-9.